JOURNAL OF MATERIALS SCIENCE: MATERIALS IN MEDICINE 11 (2000) 725–741

The processing and characterization of animal-derived bone to yield materials with biomedical applications. Part II: milled bone powders, reprecipitated hydroxyapatite and the potential uses of these materials

G. S. JOHNSON, M. R. MUCALO*
Chemistry Department, University of Waikato, Private Bag 3105, Hamilton, New Zealand
E-mail: m.mucalo@waikato.ac.nz

M. A. LORIER
MIRINZ Food Technology and Research Ltd, P.O. Box 617, Hamilton, New Zealand

U. GIELAND, H. MUCHA
Institut fuer Verbundwerkstoffe, Chemnitz Technical University, Erfenschalger Str. 73, D-09125, Chemnitz, Germany

Further studies on the processing and use of animal-bone-derived calcium phosphate materials in biomedical applications are presented. Bone powders sourced either from the direct crushing and milling of bovine, ovine and cervine bone or after being subjected to defatting and acid digestion/NaOH reprecipitation and sodium hypochlorite hydrogen peroxide treatment of animal bones were characterized using Fourier transform infra-red (FTIR) spectroscopy, ^{13}C solid state magic angle spinning (MAS) nuclear magnetic resonance (NMR) spectroscopy, atomic absorption (AA) and inductively coupled plasma (ICP) spectrometric techniques. Bone powders were trialled for their potential use as a substrate for phosphine coupling and enzyme immobilization as well as a feedstock powder for plasma spraying on titanium metal substrates. Results indicated that enzyme immobilization by phosphine coupling could be successfully achieved on milled cervine bone with the immobilized enzyme retaining some activity. It was found that the presence of impurities normally carried down with the processing of the bone materials (viz., fat and collagen) played an important role in influencing the adsorbency and reactivity of the powders. Plasma spraying studies using reprecipitated bovine-derived powders produced highly adherent coatings on titanium metal, the composition of which was mostly hydroxyapatite ($Ca_{10}(PO_4)_6(OH)_2$) with low levels of α-tricalcium phosphate ($\alpha - Ca_3(PO_4)_2$) and tetracalcium phosphate ($Ca_4P_2O_9$) also detected. In general, animal derived calcium phosphate materials constitute a potentially cheaper source of calcium phosphate materials for biomedical applications and make use of a largely under-utilized resource from abattoir wastes.

1. Introduction

The basic calcium phosphate, hydroxyapatite (HAP) has uses spanning many diverse areas. One major use of HAP is in the biomedical area as a prosthesis material because of its biocompatibility with human bone tissue [1]. Bone grafting is commonly used in orthopaedic surgery, is becoming increasingly frequent in dental surgery for the reduction of dental pouches and is also useful in plastic surgery for the repair of body defects [2]. The use of xenograft materials incorporating HAP from synthetic sources as an alternative to autologous implant materials is a burgeoning area of research worldwide.

However, HAP powder produced from synthetic procedures can be very costly. HAP must meet severe quality control criteria if it is to be used in biomedical applications. Some of the criteria are: low levels of impurity contamination (<50 ppm heavy metals) [3], precise chemical composition (Ca : P ratio $= 1.67$–1.76, single phase ($>95\%$ HAP) and satisfactory mechanical performance [4]. Waste animal bone is a potentially useful

*Author to whom all correspondence should be addressed.

and low cost source of natural HAP. Previously, [5] it was described how bovine cancellous bone could be processed to form a shape-modifiable exnograft implant material. This report will describe the processing of abattoir animal bone into milled bone and reprecipitated HAP powders and discuss experiments where the powders have been used as enzyme immobilization substrates and feedstocks for plasma spraying onto titanium metal plates.

2. Experimental

2.1. General reagents and solutions

Solvents and reagents employed in this study were used as received without further purification. Fluka brand HAP and tricalcium phosphate (TCP) were used as standards. Bleaching solutions used were industrial grade (25%) sodium hypochlorite (NaOCI) solution and 50% hydrogen peroxide (H_2O_2) solution and were obtained from Hamilton Chemicals. Isopropyl alcohol (IPA) was drum grade and also obtained from Hamilton Chemicals. All other solvents (e.g. ethanol, methyl acetate etc) were BDH Anala-R grade.

2.2. Instrumentation

Infra-red (IR) spectra over the range 4000–400 cm^{-1}, of powdered bione specimens were recorded as KBr discs on a Digilab FTS-40 FTIR spectrometer. ^{31}P and ^{13}C solid state NMR spectra (of powdered samples packed in 7 mm zirconia rotors spinning at 4.5 KHz) were acquired on a Bruker AC-200 NMR spectrometer equipped with a solid state probe, cross-polarization/magic angle spinning accessory and high power decoupling sequence for ^{31}P. ^{31}P spectra were referenced to 85% H_3PO_4 (0 ppm) using KH_2PO_4 (5.3 ppm) as a secondary external reference and a line broadening factor of 20 Hz in the Fourier transform process. All ^{13}C solid state NMR spectra were referenced to tetramethylsilane (0 ppm) using adamantane (38.3 ppm) as a secondary external reference. Any ^{31}P NMR spectra recorded of solutions were obtained using a Bruker AC300 NMR spectrometer at 121.5 MHz.

U.V./V is spectra were recorded on a Cary 1 ultra-violet/visible spectrophotometer while enzyme assay monitoring was carried out using a GBC 918 ultra-violet/visible spectrophotometer at a wavelength of 253 nm. Electron micrographs were acquired using a Hitachi S4000 scanning electron microscope (SEM) of samples affixed to sample stubs. EDX analyses for deducing Ca : P ratios were performed using Kevex Quanter software and a certified HAP standard for calcium and phosphorus quantification. Power X-ray diffractograms were performed on a Phillips X'pert PW3050/θ - 2θ diffractometer using CuKα radiation and the 2θ sampling technique. Scans were acquired between 6.0° and 150.0° 2θ using a step size of 0.030°. The acquisition time per step was set to 1.5 s. Diffracton patterns were analyzed using PC-APD diffraction libraries.

Preparation of samples for analyses by ICP and AA involved digestions of solid material in a standard 2 : 5 $HClO_4$: HNO_3 mix which were then diluted to the appropriate optimum analytical range for each element. A standard pasture sample known as ''86P'' consisting of dried, homogenized grass and extensively characterized by the Soil Fertility Service, Ruakura Agricultural Center, Hamilton, was used as a certified in-house reference material. The instrumentation used for the analysis of the bone and standard calcium phosphate samples was a Thermo Jarrell Ash IRIS axial plasma inductively coupled plasma optical emission spectrometer (for analysis of Ca, P, Na, Mg, Zn and Al) and a Perkin Elmer 5100 PC atomic absorption spectrometer (Cd, Pb and K). For the ICP measurements, plasma argon flow rates of 17 l min^{-1}, auxiliary argon flow rates of 0.5 l min^{-1}, nebulizer argon pressures of 32 psi, radio-frequency powers of 1150 Watts, and sampler flow rates of 2.4 ml min^{-1} were used in typical runs.

2.3. Source of bone and bone processing/analysis methods

Bovine bones were usually sourced from Ministry of Agriculture and Fisheries (MAF)-approved abattoirs. Ovine bone and cervine bone was sourced from supermarket sheep offcuts and MAF-approved deer abattoirs respectively. A crude bulk starting material known as ''MIRINZ Reprecipitated Bone Powder'' was prepared by cutting bovine bone into small pieces with a band saw and adding to heated water in a 200 l stirred vat to remove tissue and fat. Food grade enzyme (alcalase 2.41) was added to break down the bone marrow and extraneous organic matter adhering to the bone surfaces. The clean bone chips were then digested in a 10-day dissolution step in 5% (v/v) hydrochloric acid (HCI) solution. Remaining undissolved bone and scum were removed by filtering the solution through three layers of muslin cloth. To this relatively clear solution with pH of 2.5, saturated calcium hydroxide ($Ca(OH)_2$) solution or sodium hydroxide (NaOH) solution was then added to reprecipitate calcium phosphate. The crude product was further purified by a repeated redigestion and reprecipitation. The powder was then washed with distilled water and freeze-dried.

In contrast, bone powder referred to as ''milled animal bone'' was prepared directly from bone without digestion/reprecipitation steps by crushing bone from sheep, deer, ostrich or cattle in a hydraulic press at 100 psi followed by pressure cooking in water at 15 psi and 100 °C for 4 h with a water change half way through to remove tissue and fat. The clean bone chips were subsequently dried for 16 h in a 105 °C oven before being ground finely to <2 mm particle size powder in a hammer mill.

Fat and protein levels (before and after bleaching treatments) in the bone materials were analyzed using gravimetric petroleum ether soxhlet extraction, differential scanning calorimetry (DSC) and modified Kjeldahl methods as described previously [5, 6].

2.4. Specific solvent and solution washing steps used for bone powders

2.4.1. Further defatting of the MIRINZ reprecipitated bone powder using organic solvents

5 g of MIRINZ reprecipitated bone powder was microwaved at high power (using an 800 W domestic microwave oven) in 100 ml of distilled water, for 90 s

after boiling point was reached. The powder slurry was then filtered under gravity (using Whatman #1 filter paper), oven-dried, resuspended in IPA solvent and then microwaved till boiling (60 sec).

2.4.2. Further defatting of milled cervine bone powder using organic solvents

20 g of milled cervine bone powder was refluxed in 100 ml of Anala-R methyl acetate for 1.5 h, filtered while still warm, rinsed with fresh methyl acetate solvent and then air-dried.

2.4.3. Treatment of milled cervine bone powder with NaOH

20 g of milled cervine bone powder was stirred in 0.1 mol L^{-1} NaOH at 40 °C for 1 h, filtered, washed with distilled water and then oven-dried.

2.4.4. Treatment of the MIRINZ reprecipitated bone powder with NaOCl or H_2O_2 solution

30 g of MIRINZ reprecipitated bone powder was stirred in 300 ml of 25% NaOCl solution for 3 days. The suspension was then filtered on a Buchner funnel using Whatman #1 filter paper, rinsed with distilled water and then oven-dried. Another bleaching experiment involved the treatment of 20 g of MIRINZ reprecipitated bone powder with 500 ml of 5% (v/v) H_2O_2 solution.

2.5. Digestion and reprecipitation procedures for bone powders

The MIRINZ reprecipitated bone powder and milled cervine bone were digested in either 5% (v/v) HCI, nitric (HNO_3), sulfuric (H_2SO_4) orthophosphoric (H_3PO_4) acid solutions using a ratio of 1g of bone sample to 10 ml of 5% mineral acid solution. The digest solutions obtained were then subjected to centrifuging (5000 rpm for 10 min), solvent extraction (in petroleum spirit), filtration by paper and sintered glass or combinations of these three techniques in order to remove insoluble components. Reprecipitation was then achieved by dropwise addition of NaOH solution to the stirred digest solution such that the pH of the solution remained above 9.0. To promote full development of the HAP precipitate, the reprecipitation was carried out at 70 °C and stirred for 3 h. The solid material was filtered using Whatman #1 filter paper on a Buchner funnel and dried in a 105 °C oven for $>$ 48h.

2.6. Application studies of the bone powders

2.6.1. Enzyme immobilization on MIRINZ reprecipitated bone powder and milled animal bone powders

The coupling reagent chosen was tris(hydroxymethyl) phosphine ($P(CH_2OH)_3$). This was synthesized *in situ* [7] by adding 5 ml of 0.032 mol l^{-1} potassium hydroxide (KOH) solution dropwise with stirring to 30 ml of a solution containing 8 g of 80% (w/w) aqueous tetrakis (hydroxymethyl) phosphonium chloride ($P(CH_2OH)_4^+Cl-$) (Albright and Wilson (UK) Ltd). Attachment of the $P(CH_2OH)_3$ to the bone powders involved taking 10 g of solid material (i.e. milled cervine, and ovine bone, cancellous bovine matrix shavings, MIRINZ reprecipitated bone powder) and adding with stirring to 16.8 ml of synthesized $P(CH_2OH)_3$ solution. This gave an experimental $P(CH_2OH)_3$: solids (w/w) ratio of *ca.* 1 : 5. During a given $P(CH_2OH)_3$ coupling experiment, 1 ml aliquots from the stirred solutions were withdrawn after 10, 15, 25 and 45 min and tested with 1 ml of aqueous 0.84 mol l^{-1} $NiCl_2 \cdot 6H_2O$ solution to ensure the $P(CH_2OH)_3$ coupling reagent was in excess. U.V./Vis. spectrophotometry was used as a qualitative monitor of free phosphine in solution. The reacted solid materials were left in solution for two hours, then filtered (with washing of the separate solids with distilled water) using Whatman #1 paper by vacuum suction. Drying was carried out in a vacuum desiccator. $P(CH_2OH)_3$ was also reacted with samples of rolled collagen foam film, derived from cow hide as well pure Fluka HAP powder, as control experiments for comparisons in the enzyme immobilization studies.

To confirm that coupling of the $P(CH_2OH)_3$ to the solid materials had taken place, 2.0 g of each dried reacted sample was added to 24 ml of distilled water and 1 ml of 0.84 mol L^{-1} $NiCl_2 \cdot 6H_2O$ solution. After 1 h, the solid material was vacuum filtered and rinsed thoroughly with distilled water. The rinsed samples were then redried in a vacuum desiccator at room temperature. For purposes of computation, it was assumed that the nickel complexed to all the reactive sites on the coupling reagent attached to the reacted solid materials. The extent of nickel uptake was measured by AA spectrometry. Samples (0.1 g) were digested in 5 ml of Aqua Regia on a hotplate for 15 min. After cooling, samples were transferred to 100 ml volumetric flasks and made up to volume. In addition to these samples, phosphine-reacted solid materials not exposed to the nickel solution as well as $NiCl_2$-treated solid materials not previously reacted with the phosphine coupling reagent, were also digested and analyzed as control samples.

The activity of trypsin, the enzyme immobilized in the trials, was assayed by a standard method described in the United States Pharmacopoeia (USP) [8]. One ''USP trypsin unit'' is defined as the activity that causes a change in the U.V./Vis. absorbance of 0.003 per minute under the conditions specified in the standard assay procedure. The number of USP trypsin units per mg for a typical sample contained inside a 1.0 cm cuvette used for U.V./Vis. spectrophotometric measurements in thus given by the following equation

$$\text{Assay USP units per cuvette} = \frac{\text{change in absorbance/min}}{0.003} \quad (1)$$

The rate of trypsin uptake by phosphine-coupled milled cervine bone powder was first studied. Successive 1 ml aliquots of trypsin standard (16 ppm) were added to 0.1 g of bone material, mixed by vortex, centrifuged with 200 µl of the solution extracted for assaying. This was

performed every 5 min over a period of 1 h. Excess trypsin (1.0 ml of 1.0 mg ml^{-1} was added after this period and the sample left for 24 h in a refrigerator at 4 °C. The bone material was subsequently washed with 0.04 mol l^{-1} sodium chloride (NaCl) solution, then with distilled water to remove any free mobile trypsin. The aqueous layer above the bone materials was also assayed to check for ''bleeding'' (the detachment of trypsin from the bone materials). The uptake study was then completed on 0.1 g of the remaining phosphine-coupled samples, (i.e. milled ovine bone, bovine matrix shavings, MIRINZ reprecipitated bone powder, Fluka pure HPA and collagen derived from cow hide) by adding 5 ml of the 16 ppm trypsin standard. The decrease in trypsin activity was monitored over a 24 h period to determine rate and amount of adsorption. Control experiments were also carried out on non-phosphine-coupled materials.

The activity of immobilized trypsin on bone samples was measured by taking 0.01 g sub-samples from the washed trypsin-coupled bone material and adding to 6 ml of N-benzoyl-L-arginine ethyl ester hydrochloride (BAEE) substrate solution in a test tube, mixing by vortex and then centrifuging. 3 ml was decanted into a quartz cuvette so that the absorbance change could be measured. The spectrometer was zeroed with the substrate solution alone in the compartment and absorbance readings taken of samples over a 15 min period. The sample solution was transferred back to the test-tube and vortex mixed between each reading to allow the immobilized trypsin to continue reacting with the BAEE substrate. The actual contact time of the substrate with the immobilized trypsin was recorded with the absorbance reading.

2.7. Plasma coating methodology

Plasma coating was carried out using a LAB PLASMA TECHNIK 1200 VPS plasma coater instrument at the Technical University of Chemnitz in Chemnitz, Germany. Using the ''as-received MIRINZ reprecipitated bone powder'' as a feedstock, coatings were applied to flat $50 \times 50 \times 2$mm 99.7% purity titanium (Ti) metal plates (Alfa-Johnson-Matthey). The plates were grit-blasted prior to coating application. The feedstock was initially sieved to give a grain size between 70 and 220 μm diameter, and stirred at 40 rpm in the raw material containment vessel prior to being gravity-fed radially through a standard vertical anode ring hole into the plasma. Three plates were plasma-coated to a depth of *ca*. 80 μm using a range of burner electrical power inputs (18, 22, 26 kW) with plasma spraying conditions (chamber pressure = 60 mBar, argon gas flow rate = 30 l min^{-1}), hydrogren gas flow rate = 35 l min^{-1}), burnen-substrate distance = 220 mm, burner movement speed = 7000 mm min^{-1}, and coating cycles = 4) being held constant. Coated plates were then analyzed *in sity* by SEM/EDX and XRD to determine crystallinity and morphological characteristics. Samples for ICP and FTIR analysis were obtained by scraping off some of the grayish coating material. Digest solutions for ICP were prepared by dissolving *ca*. 50 mg of coating material in a $HClO_4HNO_3$ mix and analyzing for Ca, P and Ti.

3. Results and discussion

3.1. Bone powders: Raw material evaluation

3.1.1. MIRINZ reprecipitated bone powder

The as-received material was creamy white in color with a coarse crumbly texture. Characterization of this material (see later sections) revealed that the powder is semi-crystalline with detectable levels of residual fat so necessitating further solvent and solution treatment.

3.1.2. Milled bovine, cervine and ovine bone powder

Fig. 1 is a photograph of the three types of animal bone powder following the crushing, pressure cooking and drying processes. Bovine-derived bone was light creamy-colored and brittle. Ovine bone was dark brown/green-colored and very brittle. The cervine bone was creamy-colored and very hard. The direct milling of these bone materials to coarse powders produced a suitable feedstock for further processing to give stoichiometric HAP. As milled powders were not subject to a digest and a reprecipitation step, the powder makeup consists of the original bone components, i.e. fat, collagen and calcium hydroxycarbonate apatite (HCA). The fat content determined by gravimetric soxhlet extraction was 0.6% for bovine bone, 0.2% for cervine bone, and 2.0% for ovine bone. These quantitative results for fat content in the milled bone correlate very well with the qualitative trends demonstrated by FTIR spectra [5].

3.2. Results from further treatment of the bone powders with defatting solvents and bleaching solutions

3.2.1. NaOCl and H_2O_2 treatment of MIRINZ reprecipitated bone powder

Treatment of the MIRINZ reprecipitated bone powder with 25% aqueous NaOCl produced a foamy solution due to the evolution of carbon dioxide from the oxidation of the residual proteinaceous and fat components in the reprecipitated powder. Eventual drying of the material produced a hard cake, which could be ground into a very fine, clean white powder. Analysis showed only a small amount of residual protein and fat but high levels of sodium ions originating from the NaOCl solution. XRD confirmed the presence of NaCl in the powders.

Treatment of the MIRINZ reprecipitated bone powder with 5% (v/v) H_2O_2 solution had a very similar effect to the 25% NaOCl solution. Chemical analysis for protein

Figure 1 Photographs of boiled and defatted cattle, sheep and deer bone (after crushing but prior to milling). From left to right, bovine bone, ovine bone and cervine bone.

levels showed a higher retention of protein matter in the bone powder relative to powders treated with NaOCl.

3.2.2. Microwave heating of the MIRINZ reprecipitated bone powder with water and IPA

Microwaving of the MIRINZ reprecipitated bone powder in water and in IPA produced similar visual results for both liquids. In each case, a milky white emulsion was observed, which filtered very slowly through the filter paper. The final dried product retained the creamy original color of the MIRINZ reprecipitated bone. Analysis also showed that fat and protein were still present but at levels reduced from that of the starting material.

3.2.3. NaOCl and H_2O_2 treatment of the milled cervine bone powder with ultrasonication

Ultrasonication of the granular milled cervine bone powder in either NaOCl or H_2O_2 solutions generally produced a fine white emulsion. The use of ultrasonication greatly reduced the time needed for bleaching to produce a clean white powder from days to hours. Clean white powders very similar in nature to those obtained from NaOCl treatment of the MIRINZ reprecipitated bone powder were generated.

3.2.4. Solvent reflux of milled cervine bone powder

Refluxing of the previously pressure-cooked and milled cervine bone with methyl acetate solvent gave a much cleaner product as indicated by the visibly more free-flowing solid granules after the reflux. This reflected removal of adhered fat from the powder which tends to give an agglomerated product.

3.2.5. NaOH treatment of milled cervine bone powder

NaOH treatment of the milled cervine bone pieces gave a lighter and more fragile product which facilitated its milling. The denaturation of collagen by NaOH is most likely responsible, although FTIR spectra of the NaOH-treated cervine bone powder did not differ significantly from that of the untreated bone fragments.

3.3. Evaluation of acid digestion and reprecipitation procedures for the bone powders

3.3.1. Acid dissolution

HCl and HNO_3 are effective digesting agents for the bone-derived materials. H_2SO_4 digestions leave insoluble solids corresponding most likely to calcium sulfate while use of H_3PO_4 interestingly led to spontaneous precipitation of a low Ca : P ratio calcium phosphate phase, which was confirmed by FTIR to be monetite ($CaHPO_4$).

3.3.2. Clean-up of acid digest solutions

The two acid digest solutions from HCl and HNO_3-aided dissolution of the bone powders were significantly different in appearance. The HCl digest solution was opaque due most likely to suspended collagen and fat. The HNO_3 digest solution, on the other hand, was bright orange in color. The orange color most likely represents the reaction products arising from oxidation of the organic moieties in the bone powders (e.g. collagen) by HNO_3. Despite this, the HNO_3 digest solution did not require a clean-up step before reprecipitation of calcium phosphate from this solution was carried out. The opaqueness of the HCl digest solution, however, meant that an additional clean-up step prior to reprecipitation of the calcium phosphate was needed. simple buchner filtration was difficult due to rapid blockage of the filter paper by organic material. Solvent extraction, on the other hand, using petroleum spirits was effective in clearing the solution but was deemed an undesirable method to use in materials destined for biomedical use. Centrifugation, a non-solvent based method, was found to be the best compromise but limited (on the laboratory scale) to only small volumes of HCl digest solution which could be treated at any one time. Centrifuging leads to a compaction of the organic material into a thick layer of collagen and fat on top of the digest solution which can be easily removed.

3.3.3. Reprecipitation of calcium phosphate from the acid-digest solutions

Reprecipitation produced a white powder from the HCl digest solution and a pale orange powder from the HNO_3 digest solution. The color in the case of the HNO_3 digest solution is due to adsorption of the orange chromophores from the solution and could not be removed by simple rinsing of the powder with water. For this reason, HCl is the acid of choice in bone powder digestions.

3.4. Characterization of the bone-derived powders

3.4.1. X-ray Diffraction (XRD)

Milled cervine bone powder examined by XRD was found (compared to the XRD patterns of crystalline Fluka HAP and TCP) to give a broad and poorly resolved pattern thus affording little structural information. This is because bone material tends to be amorphous in nature as shown by previous workers who characterized bone from various animal species by XRD [9]. Broad, poorly resolved patterns were also observed for the MIRINZ reprecipitated bone powder. However, powders from further acid digestion/NaOH reprecipitation of the MIRINZ reprecipitate bone powder gave sharper XRD patterns thus indicating increased crystallinity (see Fig. 2 a and b). Additional features observed not related to the main HAP phase in X-ray diffractograms of the chemically digested/treated/reprecipitated bone powders were found [10] to be due to NaCl which serves to explain the elevated sodium levels detected in NaOH reprecipitated and NaOCl-treated powders.

Acid digestion and reprecipitation effectively converts the greater part of the bone hydroxycarbonate apatite into

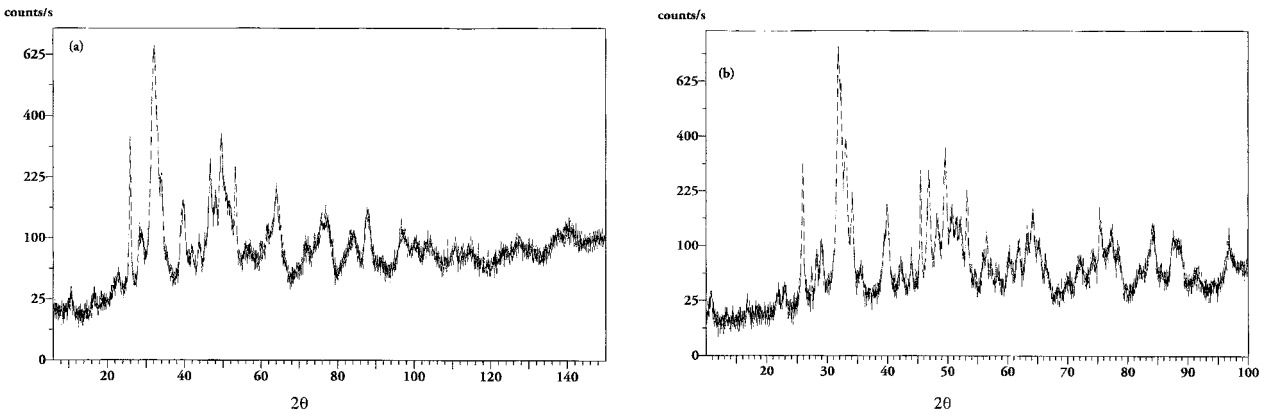

Figure 2 XRD spectra of (a) as-received MIRINZ reprecipitated bone powder, and (b) HCI digested NaOH reprecipitated MIRINZ reprecipitated bone bowder.

calcium HAP. Phase purity of calcium phosphate phases formed by precipitation is controlled by the pH of the precipitating medium [3]. Maintenance of pH at 7–9 during the precipitation ensures that HAP ($Ca_{10}(PO_4)_6(OH)_2$) will be the dominant final product. Precipitation at lower pH (i.e. 5–6) will otherwise lead to brushite ($CaHPO_4 \cdot 2H_2O$) as the dominant phase. In the present study, both the HCl-digested and the HNO_3-digested reprecipitated bone powders gave XRD patterns indicating HAP as the major phase.

3.4.2. FITIR and solid state NMR characterization of milled and reprecipitated animal-derived bone powders

Spectral characterization of *milled* animal bone by FTIR and solid state NMR spectrometry has already been covered in an earlier paper [5]. In the present report, characterization of calcium phosphate materials derived primarily from acid digestion/reprecipitation and other chemical treatments (e.g. NaOCl, H_2O_2 and NaOH treatments) is reported. The materials subjected to digestion/reprecipitation were MIRINZ reprecipitated bone powder and milled cervine bone.

3.4.3. Spectral characterization of the as-received MIRINZ reprecipitated bone powder

Fig. 3(a) is an FTIR spectrum of a KBr disk of as-received MIRINZ reprecipitated bone powder. The spectrum shows peaks typical of an apatitic calcium phosphate phase as evidenced by the strong peack observed at 1032 cm^{-1} due to the asymmetric P–O stretching mode of PO_4^{3-} and the two peaks of medium intensity appearing at 564 and 603 cm^{-1}, which are due to PO_4^{3-} bending modes. It is also evident from weak peaks observed at 1459, 1420 and 875 cm^{-1} that a small amount of carbonate is present, possibly substituted in the HAP lattice either in the position normally occupied by -OH in HAP ($Ca_{10}(PO_4)_6(OH)_2$, i.e. A-type carbonate) or in the position occupied by PO_4^{3-} (B-type carbonate). In addition, weak peaks at 2961, 2927 and 2856 cm^{-1} indicate that hydrocarbons (possibly from residual fat traces) are present in the powder. A broad peak at 3434 cm^{-1} and an associated weak peak at 1655 cm^{-1} also show traces of moisture in the reprecipitated bone powder. The ^{13}C solid state NMR of the as-received MIRINZ reprecipitated bone powder (Fig. 4(a)) features a strong peak at 30 ppm with associated weak peaks at 22.8 and 13.0 ppm. These can be assigned to long chain alkane carbons contained in the residual fat in the powder [11]. An aditional weak peak can also be observed at 130.3 ppm. This is believed to be a resonance arising from the presence of a small amount of monounstaurated fatty acids (e.g. linoleic acid) which occur in beef tallow. The level of this is probably low (i.e. $>1\%$) as no band intensity above 3000 cm^{-1} (this being indicative of the presence of alkenic C–H

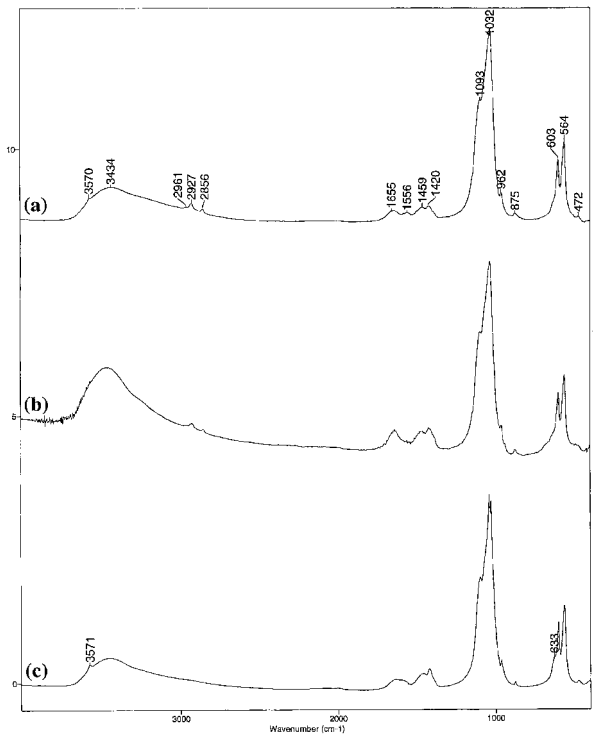

Figure 3 FTIR spectra of (a) as-received MIRINZ reprecipitated bone powder (b) NaOCl-treated MIRINZ reprecipitated bone powder and (c) HCl digested NaOH reprecipitated ''MIRINZ reprecipitated bone powder''.

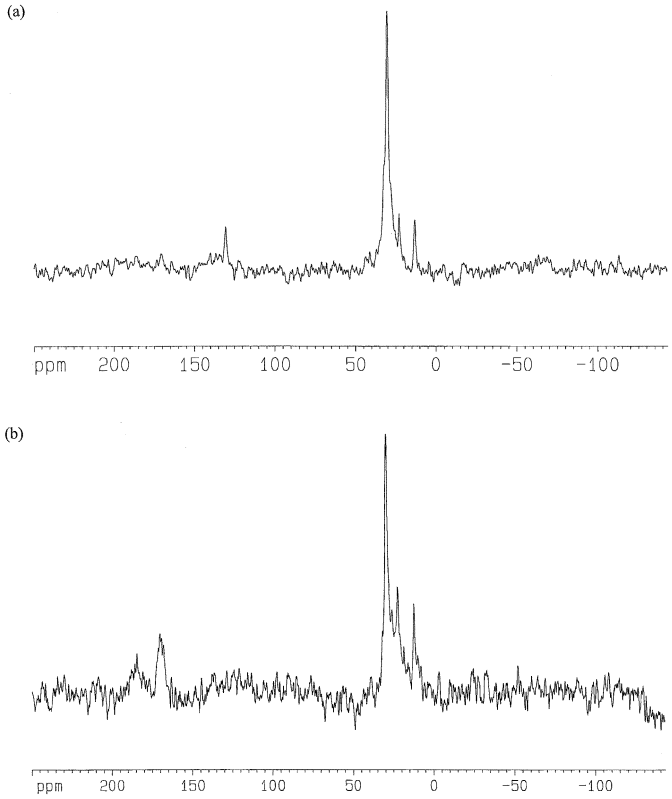

Figure 4 ^{13}C; solid state MAS NMR spectra of (a) as-received and (b) NaOCl-treated MIRINZ reprecipitated bone powder.

stretching) in the FTIR spectrum of the MIRINZ reprecipitated bone powder is discernible. The solid state NMR also features a very weak peak at 170.6 ppm. This can be unequivocally assigned go the ^{13}C resonance of carbonate and agrees with IR data which demostrate the presence of carbonate in the power. ^{31}P solid state NMR spectra of the powder show a single resonance centered at 4.28 ppm. The shape and simplicity of the resonance indicated that P resides in an apatitic phosphate-type environment. This peak tends to be invariant in appearance in spectra of different bone powders and so is of limited value in characterization.

3.4.4. MIRINZ reprecipitated bone powder treated with water, IPA, NaOCl or H_2O_2 solution

Microwaving of the MIRINZ reprecipitated bone powder in distilled water of IPA produced little change in the FTIR spectra apart from a small decrease in the intensity of the C-H stretching peaks at 2900–3000 cm^{-1} (in the case of the IPA-washed sample) due to fat. The only change noticeable in ^{13}C solid state NMR spectra of samples after water or IPA microwaving was a reduction in intensity of the weak 130 ppm resonance assigned to monounsaturated fatty acid residues.

Fig. 3(b) is an FTIR spectrum of NaOCl-treated MIRINZ reprecipitated bone powder. Fig. 4(b) is the corresponding ^{13}C solid state NMR spectrum. NaOCl treatment appears to lead to elevated levels of carbonate in the reprecipitated bone powders as evidenced by the increase in relative intensity of 1466, 1420 and 875 cm^{-1} peaks relative to the main phosphate peaks in the FTIR spectrum. This is likely to arise from the fact that the NaOCl solution is at a basic pH [5] so that atmospheric CO_2 could enter the solution, become converted to carbonate, and thus enter the apatitic calcium phosphate structure during soaking. The ^{13}C solid state NMR spectrum of the NaOCl-trated bone powder (Fig 4(b)) supports the FTIR observation of increased carbonate levels as a noticeable carbonate peak at 170.2 ppm can be observed. A weak resonance observed at 184.4 ppm is probably due to the carboxyl carbon on straight chain alkane fatty acids. It is likely that soaking of the bone powder in the NaOCl medium may have led to the formation of some insoluble fatty acid salts which are not easily removed. This is supported by the observation of hydrocarbon-associated peaks 2963, 2926, and 2855 cm^{-1} in the FTIR spectrum and long chain alkane carbon-associated resonances at 12, 22.6 and 29.7 ppm in the ^{13}C solid state NMR spectrum (see Fig. 4 (b)).

H_2O_2 treatment of the MIRINZ reprecipitated bone powder does not lead to an increase in carbonate content (carbonate levels appear, in fact, to be unaffected by the treatment). Hydrocarbon content is reduced but not eliminated altogether so that the result is very similar to that obtained for NaOCl-soaked MIRINZ reprecipitated bone powder. The ^{13}C solid state NMR spectrum of H_2O_2-treated MIRINZ reprecipitated bone powder reflects the features observed in the FTIR, namely low carbonate content. Resonances at 12.6, 22.9 and 30.0 ppm as well as a weak peak at 184.8 ppm show that residual long chain fatty acids are still present in the powder after treatment.

3.4.5. HCl-digested and reprecipitated MIRINZ bone powder

Fig. 3(c) is an FTIR spectrum MIRINZ reprecipitated bone powder which had previously been redissolved in HCl and then reprecipitated with NaOH solution. The FTIR spectrum reveals that the HCl digestion/reprecipitation process was extremely efficient in eliminating the fatty hydrocarbon residues from the bone powder. ^{13}C solid state NMR spectra of the sample were very noisy and featured very weak features showing effective removal of carbonaceous species. Carbonate levels were, however, enhanced relative to the as-received MIRINZ reprecipitated bone powder indicating uptake of carbonate during the reprecipitation process in NaOH solution. This was confirmed by the observation of a weak resonance at *ca.* 170 ppm in the 13C solid state NMR spectrum of the powder.

3.5. Studies on milled cervine bone powder

3.5.1. Milled cervine bone as-received (after boiling and after methyl acetate or NaOH treatment

Fig. 5(a) is an FTIR spectrum of milled cervine bone and represents the state of the bone after prior boiling to remove the bulk of the fat and other extraneous matter. The spectrum is that typically obtained for a natural bone specimen and shows the usual hydroxycarbonate apatite-associated features at 1459, 1412, 1032, 872, 603 and 562 cm^{-1} as well as features due to collagen and moisture (3426, 3071, 2931, 2879, 1655 and 1546 cm^{-1}). Fat levels in the specimen are low in this sample as evidenced by the absence of any sharp C–H stretching bands which would be superimposed on the broader collagen-associated C–H stretching bands in the 2879–3071 cm^{-1} region. This is partially confirmed in the ^{13}C solid state NMR spectrum (Fig. 6(a)) which is mostly dominated by resonances attributable to collagen, although a sharp peak at *ca.* 30 ppm superimposed on the broad collagen-associated alkane-associated C resonances as well as a broad peak at 130 ppm suggested some residual fat content (in the form of saturated and monounsaturated long chain fats) in the cervine bone. FTIR spectra of crushed cervine bone after boiling and subjected to methyl acetate or NaOH treatment were virtually identical to that given by the untreated milled cervine bone after boiling. ^{13}C solid state NMR spectra of the NaOH- and methyl acetate-treated bone were also similar except that the NaOH- treated cervine bone gave peaks of moderate to weak intensity at 130 and 117 ppm indicating some monounsaturated fatty acid salts that had formed possibly by base-catalyzed hydrolysis of residual fatty acid esters and precipitated as insoluble salts under the basic conditions.

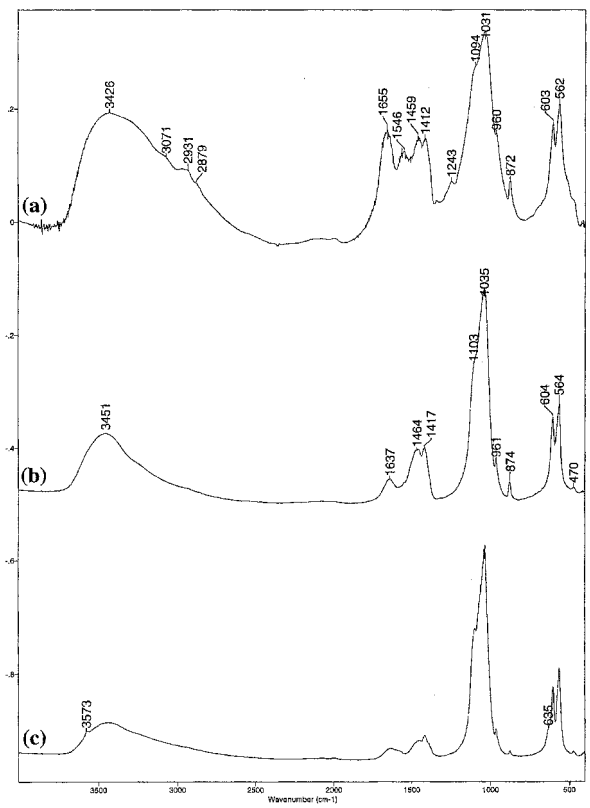

Figure 5 FTIR spectra of (a) milled cervine bone (after boiling), (b) NaOCL-treated milled cervine bone and (c) HNO_3-digested NaOH-reprecipitated milled cervine bone.

3.5.2. NaOCl-treated milled cervine bone

Fig. 5(b) is the FTIR spectrum of a sample milled cervine bone after boiling that had been treated using NaOCl. It is apparent from the FTIR spectrum that NaOCl treatment has effectively removed much of the collagenous and fatty hydrocarbon component of the milled cervine bone but left carbonate largely intact as evidenced by the significant peak intensity at 1464, 1417 and 873 cm^{-1} due to carbonate substituted in the apatitic calcium phosphate strcture. This is also reflected in the ^{13}C solid state NMR spectrum (Fig. 6(b)) which was generally clear of ^{13}C-associated resonances save for a weak peak at 168 ppm due to carbonate. Indeed, in our previous study [5] on NaOCl treatment of intact bovine bone matrices, carbonate was found to remain after NaOCl treatment.

3.5.3. Cervine bone reprecipitated after acid digestion in HCl, HNO_3 and H_3PO_4

Fig. 5(c) is an FTIR spectrum of cervine bone digested in HNO_3 and then reprecipitated in NaOH solution. The spectrum indicates that HNO_3, like HCl in the case of the MIRIINZ reprecipitated bone powders, is extremely effective at removing fat and collagen impurities from the milled cervine bone powders. However, instead of a pristine white powder as was produced from reprecipitation of HCl-digested samples, a yellow-colored solid was obtained, which was very difficult to decolorize. Thus as found with the MIRINZ reprecipitated bone powders, HCl digestions gave the cleanest powders with significant removal of fat and collagen. Carbonate (as indicated by FTIR and ^{13}C solid state NMR) was, however, still present, and was probably reintroduced into the powder during its reprecipitation from alkaline solution.

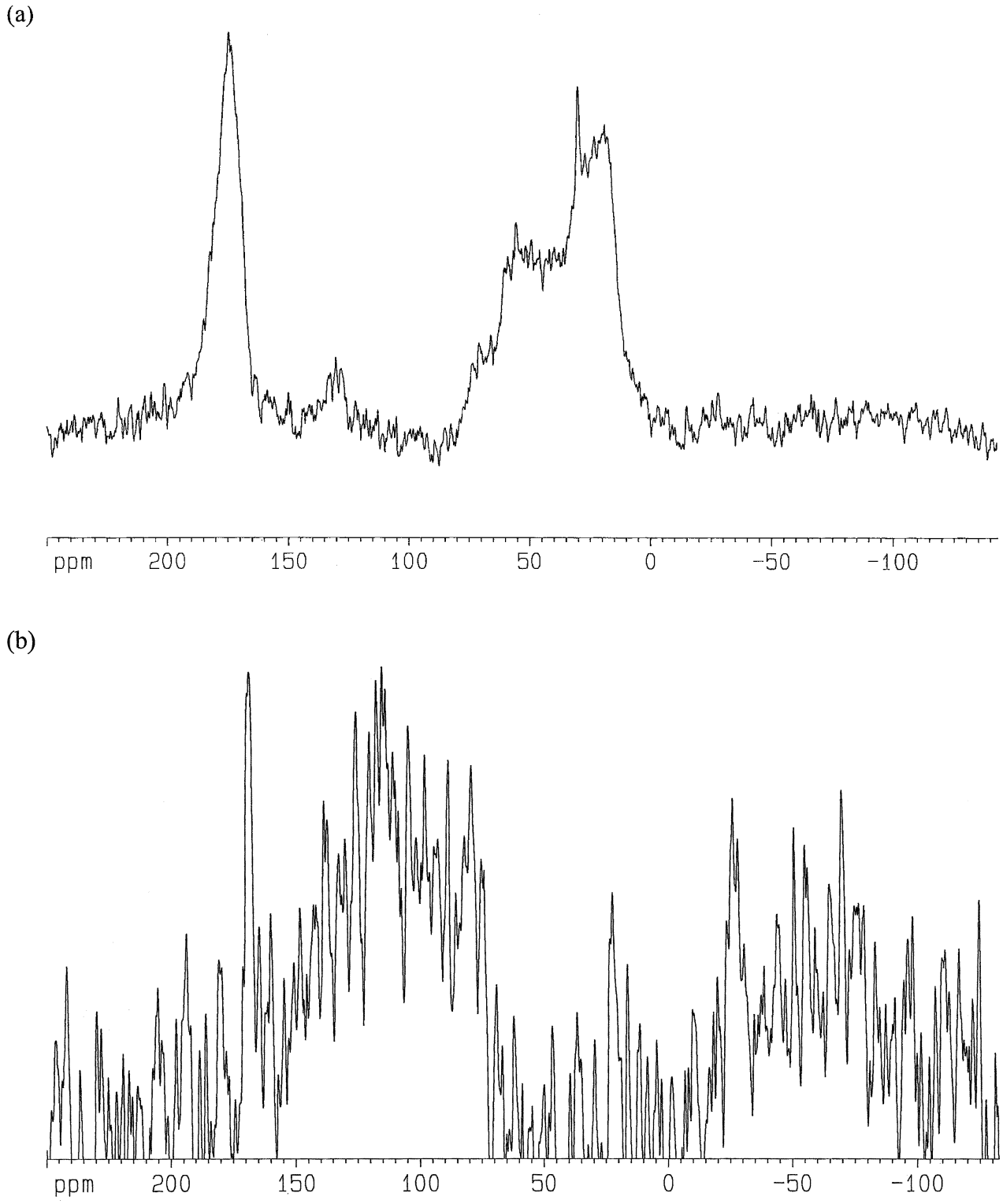

Figure 6 ^{13}C solid state MAS NMR spectra of (a) milled cervine bone (after boiling) and (b) NaOCl-treated milled cervine bone.

H_3PO_4-digestion and reprecipitation of as-received MIRINZ bone powder led not to HAP but to monetite ($CaHPO_4$) as detected by FTIR spectroscopy. Using H_3PO_4 causes a large change in molar Ca : P ratio in the digest solution which may influence phase evolution during precipitation. The result is surprising given that monetite precipitate should hydrolyze to HAP in basic solution. It is possible that the maturation period was not long enough to effect the phase transition.

3.6. Comparison of the organic (fat) levels in the bone powders using differential scanning calorimetry (DSC)

In our earlier work on processing of bone matrices [5], the thermal transitions resulting from heating of the bone material were discussed. In the MIRINZ reprecipitated bone materials (plus subsequently processed samples of this material), the exothermic fat combustion transition stage peak, which was observed in the temperature range

300–400 °C, was integrated and the numbers obtained were compared between samples in order to assess the effect of subsequent treatments on the bone powders on the degree of fat removal. In general, the peak positions observed for samples were consistent to ± 0.5 °C with peak areas being reproducible to $\pm 5\%$. Table I summarizes the peak positions and integrals for the exothermic fat combustion peak in the 300–400 °C temperature range for the samples analyzed.

From the results, it is apparent that microwaving of the as-received MIRINZ reprecipitated bone powder in water in water or IPA does not change the fat levels to any detectable extent. Treatment with NaOCl or H_2O_2 causes significant (but not complete) fat removal with NaOCl being a relatively more effective fat removal medium than H_2O_2. Generally, digestion of the MIRINZ reprecipitated powder or milled cervine bone powders in HCl and HNO_3 followed by reprecipitation in NaOH proved to be the best methods for removing the smallest residual fat traces. Powders processed in this manner gave the lowest integrals in the DSC (see Table I) with HNO_3 being most effective as a fat removal agent.

3.7. ICP and AAS spectrometric analyses of the bone powders concentrations of the major elements present in the bone powders and the effect of washing and chemical treatments

Table II summarizes the ICP and AAS-determined concentrations (in wt %) for the major elements present in the bone powder specimens studied. Commercial HAP and TCP samples were also analyzed for comparison. Results obtained for milled cervine, bovine and ovine bone (after boiling) have already been reported in an earlier paper [5], the results for milled cervine bone after boiling are reiterated in Table II for comparison with subsequent washing and chemical treatments carried out on the milled cervine bone powder.

3.7.1. MIRINZ reprecipitated bone powder

The sodium level in the crude MIRINZ reprecipitated bone powder is relatively high which is a direct consequence of the use of NaOH in the reprecipitation process and reflects salt (NaCl) impurities. Washing processes such as microwaving in water or in IPA serve to remove much of this sodium contamination as reflected by the lower wt % values obtained (see Table II). Levels of magnesium varied little with washing, NaOCl or H_2O_2 treatment. Differences in magnesium levels between different samples were paralleled by corresponding changes in the calcium concentrations indicating that the magnesium was a structural component of bone. It was interesting to note that the molar Ca : P ratio in washed/chemically treated bone powder samples was significantly different from that of the as-received MIRINZ reprecipitated bone powder. In all cases, chemical treatment or simply microwaving in water or IPA solvent served to give a powder with a higher Ca : P ratio relative to the original powder. This suggests the presence of soluble calcium phosphate compounds in the crude MIRINZ powder which dissolve and reprecipitate to form the more thermodynamically stable, calcium rich phase of calcium HAP (stoichiometric molar Ca : P ratio = 1.67). However, some caution must be exercised in the interpretation of changes in Ca : P ratio, as a higher Ca : P ratio could also mean lower phosphate due to greater incorporation of carbonate by substitution for phosphate in the calcium HAP structure (i.e. B-type carbonate substitution). This incorporation could occur during the chemical treatment or solvent wash process if no special or stringent precautions have been taken to isolate the system from the atmosphere. In addition, ICP does not distinguish between organic or inorganic P so that washing out of organic phosphate compounds from the bone materials may also lead to changes in the analyzed Ca : P molar ratio.

3.7.2. Milled cervine bone powder

Milled cervine bone powder (after boiling) show typically very low sodium levels (see Table II). However, treatments involving either NaOCl or NaOH lead to increases in sodium levels. Molar Ca : P levels are typically high in the cervine derived bone powders (Ca : P = 1.76–1.90). This is directly attributable to the higher natural carbonate content in these materials as attested by FTIR and ^{13}C solid state NMR spectra.

3.8. Trace element analysis of the bone powders and the effect of washing and chemical treatments

Table III summarizes the trace element analyses on the bone powders before and after the various solvent and chemical treatments. The only significant trend of interest in this data is the large reduction in potassium

TABLE I Peak position and computed integrals for the exothermic peak corresponding to fat combustion in DSC analyses of the MIRINZ reprecipitated bone powders as-received and after various processing treatments

Sample description	Peak maximum (°C)	Integral
MIRINZ reprecipitated bone powder as-received (Pdrl)	324.4	1419
Pdrl + water microwave	338.7	1534
Pdrl + IPA microwave	329.8	1382
Pdrl + NaOCl treatment	317.2	931
Pdrl + H_2O_2 treatment	328.1	1072
Pdrl + HCl digestion/NaOH reprecipitation	307.6	202
Milled cervine bone (after boiling)	379.2	2840
Milled cervine bone + HNO_3 digestion/NaOH reprecipitation	322.5	36

TABLE II Concentrations of the major elements in bone powder and standard calcium phosphate samples as measured by ICP. Uncertainties in concentration are ± 5%

Sample	Na (%)	Mg (%)	Ca (%)	P (%)	Ca : P ratio
Fluka HAP	0.007	0.007	40.0	19.0	1.63
Fluka TCP	0.075	0.16	38.1	20.9	1.41
MIRINZ reprecipitated bone powder (as-received) (Pdrl)	7.09	0.25	27.5	13.9	1.53
Pdrl + water microwave	0.90	0.30	31.0	14.1	1.70
Pdrl + IPA microwave	1.28	0.30	31.0	13.9	1.72
Pdrl + NaOCl treatment	6.50	0.26	26.0	12.1	1.66
Pdrl + H_2O_2 treatment	0.70	0.31	32.0	14.4	1.72
Pdrl + HCl digestion/NaOH reprecipitation	9.50	0.23	24.0	11.0	1.69
Milled cervine bone (after boiling) (Pdr2)	0.58	0.39	26.0	10.6	1.90
Pdr2 + methyl acetate reflux	0.58	0.38	26.0	11.0	1.83
Pdr2 + NaOH treatment	0.95	0.40	26.0	11.0	1.83
Pdr2 + NaOCl treatment	3.30	0.38	30.0	12.9	1.80
Pdr2 + HCl digestion/NaOH reprecipitation	4.60	0.45	30.0	13.2	1.76
Pdr2 + HNO_3 digestion/NaOH reprecipitation	1.10	0.50	34.0	14.3	1.84

from 300 ppm in the as-received MIRINZ reprecipitated bone powder and from 120 ppm in the milled cervine bone powder (after boiling) to concentrations of 30–60 ppm after microwaving in water or IPA, NaOCl or H_2O_2 treatment and acid-digestion/reprecipitation processes. This indicated that potassium is reversibly held in these materials and is thus easily removed. Levels of Cd, Pb and Al in the powders were generally at or below the respective detection limits for these elements. The negligible levels of heavy metal contaminants mean that such materials are suitable in such applications as nutritional supplements or in biomedical applications such as feedstocks for plasma spraying, and enzyme immobilization supports.

3.9. Application studies of the bone powders

3.9.1. Enzyme immobilization on MIRINZ reprecipitated bone powder and milled animal bone

3.9.1.1. The use of $P(CH_2OH)_3$ *versus Glutaraldehyde as a coupling agent.* Tris(hydroxymethyl)phosphine ($P(CH_2OH)_3$) was employed to immobilize enzymes onto the surfaces of bone-derived materials in this study. The $P(CH_2OH)_3$ must be used quickly after its formation as it oxidizes to phosphine oxide on exposure to air. ^{31}P liquid NMR spectroscopy was thus employed to confirm the integrity of the generated $P(CH_2OH)_3$ before it was used in experiments. Ni^{2+} ion is also know to complex strongly with two molecules phosphine giving a square planar complex exhibiting an intense orangecolor. Confirmation of the formation of the phosphine can also be made by adding aqueous $NiCl_2 \cdot 6H_2O$ to the prepared $P(CH_2OH)_3$.

As an enzyme coupling reagent, $P(CH_2OH)_3$ is recognized as being better than the more commonly used glutaraldehyde, which has the undesirable property of continually polymerizing upon storage and a tendency to exhibit reversibility of the Schiff base it forms upon coupling with functional groups (e.g. $-NH_2$) on the support [7]. The $P-CH_2-OH$ groups on $P(CH_2OH)_3$ undergo Mannich-type condensation reactions at room temperature with N–H group-containing compounds, giving aminomethyl phosphines, $-P-CH_2-N$ [12]. The use of $P(CH_2OH)_3$ as a coupling agent has additional

TABLE III Concentrations of the trace elements in bone powder and commerical calcium phosphate samples as measured by ICP and AAS elemental analysis techniques

Sample	K (ppm)	Zn (ppm)	Cd (ppm)	Al (ppm)	Pb (ppm)
Fluka HAP	< 10[a]	53	1.07	27	< 3[b]
Fluka TCP	30	10	< 0.2[c]	128	< 3
MIRINZ reprecipitated bone powder (as-received) (Pdr1)	300	161	< 0.2	< 20[d]	< 3
Pdrl + water microwave	40	190	< 0.2	70	40
Pdr1 + IPA microwave	40	200	< 0.2	< 20	3.0
Pdr1 + NaOCl treatment	40	200	< 0.2	< 20	4.0
Pdr1 + H_2O_2 treatment	30	190	< 0.2	< 20	< 3
Pdrl + HCl digestion/NaOH reprecipitation	60	140	< 0.2	< 20	< 3
Milled cervine bone (after boiling) (Pdr2)	120	77	< 0.2	< 20	< 3
Pdr2 + MeOAc reflux	130	77	< 0.2	< 20	< 3
Pdr2 + NaOH treatment	60	79	< 0.2	< 20	< 3
Pdr2 + NaOCl treatment	60	99	< 0.2	< 20	4.0
Pdr2 + HCl digestion/NaOH reprecipitation	40	102	< 0.2	< 20	4.0
Pdr2 + HNO_3 digestion/NaOH reprecipitation	10	109	< 0.2	< 20	4.0

[a]The detection limit for K = 10 ppm (when analyzed by AAS).
[b]The detection limit for Pb = 3 ppm (when analyzed by AAs).
[c]The detection limit for Cd = 0.2 (when analyzed by AAS).
[d]The detection limit for Al = 20 ppm (when analyzed by ICP).

advantages [7, 13–15] including an increase in the number of immobilizing groups, together with an improved hydrolytic stability of the resultant $P-CH_2-$ N-enzyme linkages over, for instance, the hydrolyzable C–N enzyme analogs formed from glutaraldehyde. Moreover, $P(CO_2OH)_3$, like glutaraldehyde, has the ideal chemical property of using non-essential $-NH_2$ groups on the enzyme so that the partial inactivation of the enzyme by immobilization is minimized.

3.9.1.2. Results from the initial preparation of the phosphine. ^{31}P solution NMR spectra of the prepared $P(CH_2OH)_3$ featured two peaks. The most intense peak was observed at -23.4 ppm and represented the $P(CH_2)OH_3$ [7]. The second peak was much smallar and centered at $+27.2$ ppm. This was assigned on the basis of previous reports [7] to unreacted phosphonium ion precursor, ($P(CH_2OH)_4^+$). Incomplete reaction of the precursor to $P(CH_2OH)_3$ is expected because the added KOH was below the stoichiometric ratio required to effect complete conversion. This is because excess KOH in the solution can cause catalytic decomposition of the $P(CH_2OH)_3$ product [16].

Addition of the generated $P(CH_2OH)_3$ to aqueous $NiCl_2$ solution resulted in a color change from green to bright orange signifying the formation of a nickel-phosphine complex. The orange color gradually fades with standing for several hours to a pale yellow liquid, due to degradation by air oxidation of the $P(CH_2OH)_3$ ligand.

3.10. Coupling to bone-derived powders

The coupling of the $P(CH_2OH)_3$ to the bone-derived powders is not an immediate process. After 45 min of stirring the $P(CH_2OH)_3$ with bone, the phosphine was still found to be in excess as extracts from the reaction solution were still observed to cause color changes when added to green aqueous $NiCl_2$ solution. A total reaction time of 2 h gave a sufficient degree of coupling. This period of reaction time was found to be suitable for complete coupling in previous studies [7, 15]. Upon being coupled with $P(CH_2OH)_3$, the bone powders took on a lighter, full bodied texture.

A quick indication of the extent of phosphine uptake (as reflected approximately by the uptake of nickel by complexation to the bound phosphine on the bone materials) could be obtained by analysis of the acid-digested sample by AAS. Table IV summarizes the results of the Ni AAs analysis. Control samples 2A, 3A, 4A and 5A show that nickel could not be detected in samples of bone material that had been phosphine-coupled but not exposed to $NiCl_2$ solution. This guarantees that any nickel observed in samples mixed thereafter in $NiCl_2$ solution is entirely sourced from that solution. The extent of phosphine uptake in the bone materials can thus be roughly estimated by assuming most of the nickel taken up adsorbs to reactive phosphine sites in the ratio of two phosphine groups to each Ni^{2+} atom. The level of phosphine uptake calculated in this manner is, however, only an approximation as it can be shown that some uptake of nickel can occur in natural bone materials in the absence of phosphine coupling as illustrated for a sample of milled cervine bone that was mixed with $NiCl_2$ solution (sample 1A, Table IV). However, when compared directly with a sample of phosphine-coupled cervine bone which was also exposed to $NiCl_2$ solution (sample 1B, Table IV), it is clear that the level of nickel uptake by the phosphine-coupled cervine bone is far greater than that for cervine bone without anchored phosphine groups.

Table IV indicates that the milled bone, (bovine) bone matrix and collagen foam samples all showed a high degree of nickel uptake, which had been enhanced by phosphine coupling. It was also evident that some phosphine can attach to pure microcrystalline HAP, albeit at significantly lower levels relative to the pure collagen and bone-derived materials. In general, collagen is recognized as being the principal coupling site for phosphine molecules which is supported by data given in Table IV for nickel uptake which was greatest in materials that had some collagen content. Assuming all nickel detected to be specifically phosphine-bound on the surface of the bone materials, the level of immobilized phosphine can thus be estimated to be from 13–17 mg/g

TABLE IV AAS–measured levels of Ni in bone materials involved in enzyme immobilization

Sample I.D.	Description	Ni/ppm	Phosphine (est.)[a]/ppm
1A	Milled cervine bone mixed with $NiCl_{2(aq)}$	1510	n/a
1B	Phosphine-coupled cervine bone[b] mixed with $NiCl_{2(aq)}$	8510	17020
2A	Phosphine-coupled bovine bone shavings	< d/1	n/e
2B	Phosphine-coupled bovine bone shavings mixed with $NiCl_{2(aq)}$	8060	16120
3A	Phosphine-coupled ovine bone	< d/1	n/e
3B	Phosphine-coupled ovine bone mixed with $NiCl_{2(aq)}$	6510	13020
4A	Phosphine-coupled collagen foam film	< d/1	n/e
4B	Phosphine-coupled collagen foam film mixed with $NiCl_{2(aq)}$	5320	10,640
5A	Phosphine-coupled pure Fluka HAP	< d/1	n/e
5B	Phosphine-coupled pure Fluka HAP mixed with $NiCl_{2(aq)}$	990	1980

[a]This is an estimated level of phosphine based on the assumption that two phosphine molecules bind to one Ni^{2+} ion. The actual amount is a little lower given that some degree of uptake of nickel by the natural bone and collagen components alone of the materials could also be occurring from the aqueous $NiCl_2$ soultion.

[b]Analysis of nickel in the phosphine-coupled cervine bone before mixing with aqueous $NiCl_2$ solution is not available.

n/a = Not applicable.

n/e = Not estimable since nickel is not present.

< d/1 = Below the detection limit for nickel (0.005 ppm).

of bone materials. The original amount of phosphine used was 200 mg per gram of bone material showing only a 6.5–8.5% uptake. A longer contact time may be required to increase the degree of uptake. The mode of $P(CH_2OH)_3$ coupling to the bone materials via the collagen is most likely to be principally through the $-NH_2$ groups. The presence of collagen in bone thus allows these materials to be potentially usefully enzyme immobilization substrates.

3.11. Trypsin coupling to the phosphine couple bone, collagen and HAP materials

Trypsin was the enzyme chosen in these studies mainly because of its availability and ease of assay. Its immobilization on collagen has also been studied by other researchers [17], which allows for comparison to be made.

3.11.1. Trypsin uptake

The absorbance at 253 nm was tested for just the BAEE substrate (no sample or trypsin added). The readings of absorbance were observed to vary randomly by $\pm$ 0006 of an absorbance unit. As a check, each set of analyses was accompanied by the assaying of a 16 ppm trypsin standard.

The first set of assays for studying the uptake of trypsin on phosphine-coupled cervine bone showed that small incremental additions became adsorbed onto the bone materials relatively quickly. The activity of the reacting solution remained relatively static at $\sim$ 0.6 USP trypsin units until the ninth addition of 16 ppm trypsin at which point the activity increased to 1.3 USP trypsin units.

On addition of 1000 ppm trypsin to the same solution, the large activity resulting ($<$*ca.* 50 USP trypsin units) exceeded the maximum limit measurable by the U.V./Vis. spectrophotometer. After refrigerating this solution for 24 h (at *ca.* 4 °C), the solution absorbance was remeasured and found to exhibit a reduced trypsin activity of 36 USP trypsin units. This indicated that the phosphine-coupled cervine bone had either taken up more trypsin or had partially denatured over the 24 h period.

After washing the 24-hour-refrigerated solution from the solid bone material and replacing the solution with distilled water only, further trypsin assays were performed to test for ''bleeding'' (mobilization/desorption of trypsin from the surface of the bone materials). The solution was found to have an activity of 0.8 USP trypsin units after *ca.* 5 min. After allowing the solution to stand (in a refrigerator) for a further 24 and 144 h (and measuring the trypsin activity after each period), activities of 2.1 and 3.2 USP trypsin units respectively were found for the 24 h and 144 h standing time periods. This indicated a slow loss of trypsin into solution, possibly of non-mobilized material. A further thorough wash and further soaking in fresh distilled water for 24 h gave a measured activity which was below the detection limit ($>$0.1 USP trypsin units) thus indicating an apparent halt to bleeding.

3.11.2. Other materials trialled

A series of experiments was undertaken for measuring enzyme uptake for the other phosphine-coupled bone, collagen and HAP materials. The results are summarized in Table V. The material that showed the best uptake of trypsin was the phosphine-coupled collagen. Over 24 h, the trypsin was almost fully immobilized from the solution, and after washing with distilled water the collagen material showed no signs of ''bleeding''. The phosphine-coupled animal bone material (bovine and ovine) showed very similar results to the phosphine-coupled collagen material. Pure crystalline (Fluka brand) HAP showed little ability to immobilize trypsin (with or without coupled phosphine) whereas the ovine and bovine bone material (without any prior phosphine coupling) appeared to take up trypsin at a similar rate to the other materials tested but showed definite signs of ''bleeding'' when the 24 h-soaked samples were washed (see Table V).

3.11.3. Activity of phosphine-coupled cervine bone with immobilized trypsin

The activity of trypsin immobilized on phosphine-coupled cervine bone, over a 15 min period in contact with the BAEE substrate is illustrated by the graph in Fig. 7. The rate of activity is observed to increase quickly in the first 3 min and then levels off before dropping slowly after 7 min. Peak activity occurred between 5 and 7 min after addition of the trypsin immobilized cervine bone sample to the BAEE substrate. These results show that the trypsin can be successfully immobilized onto bone materials (preferably with residual collagen in the matrix) without losing its enzyme functionality.

TABLE V Assay results for experiments involving trypsin immobilization on various materials in USP trypsin units

Sample I.D.	Sample description	Activity after 80 ppm trypsin added to 0.1 g of material (numbers in brackets refer to soaking time of sample)	Activity after washing (24 hour soaked) sample
A	Fluka HAP	7.6 (5 min), 6.33 (24 h)	$<$ 0.1
B	Fluka HAP + phosphine	7.05 (5 min), 6.0 (24 h)	$<$ 0.1
C	Collagen + phosphine	6.83 (5 min), 3.97 (1 h), 0.50 (24 h)	$<$ 0.1
D	Bovine bone + phosphine	7.13 (5 min), 6.90 (1 h), 0.93 (24 h)	$<$ 0.1
E	Ovine bone + phospine	4.90 (5 min), 3.90 (1 h), 0.70 (24 h)	$<$ 0.1
F	Bovine bone	4.87 (5 min), 2.77 (1 h), 1.00 (24 h)	0.20
G	Ovine bone	6.37 (5 min), 1.40 (24 h)	$<$ 0.40

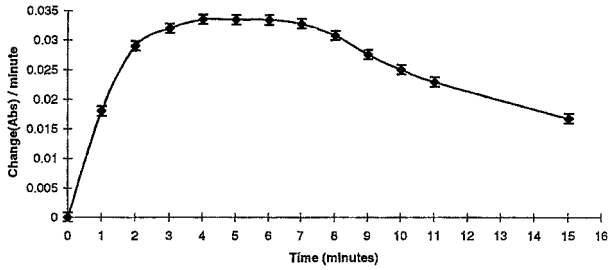

Figure 7 Plot of change in absorbance per minute at 253 nm versus time for a phosphine-coupled cervine bone sample on which trypsin had been previously immobilized. The bone sample was immersed in a BAEE substrate solution.

3.12. Use of the bone powders as a feedstock in plasma spraying: Preliminary trials

Preliminary trials on the use of reprecipitated bone powder as a plasma coating feedstock were carried out on the as-received MIRINZ reprecipitated bone powder. Best results were obtained when the feedstock powders were pre-sieved to fall within the 70–220 μm particle size range. The presence of particle ''fines'' smaller in size than 70 μm did not have optimum flow through the vertical anode ring hole in the plasma sprayer apparatus, so leading to clogging.

The resulting coatings made on 3 Ti plates using different burner electrical power inputs (18, 22, 26 kW) exhibited a coarse, adherent uniform gray colored surface (see Fig. 8) and were similar in appearance except for a slight intensification of the color for coatings prepared at higher electrical input powers. No surface cracking was observed in any of the coatings. SEM analysis of the coatings revealed similar morphological characteristics in all three plates. However, XRD analysis indicated that the actual phase of the calcium phosphate in the MIRINZ reprecipitated bone powder had undergone some transformations induced by the conditions under which the plasma spraying was carried out.

3.12.1. XRD analysis of the coated plates

In situ XRD analysis of the coating material on each plate gave broadly similar patterns. Fig. 9 is an XRD pattern

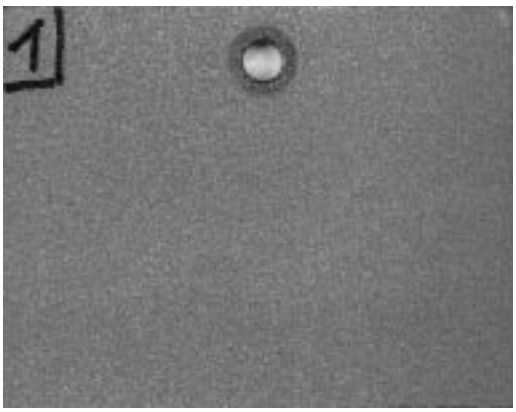

Figure 8 Photograph of a plasma sprayed Ti plate prepared at 18 kW electrical input power using the pre-sieved as-received MIRINZ reprecipitated bone powder as a feedstock powder.

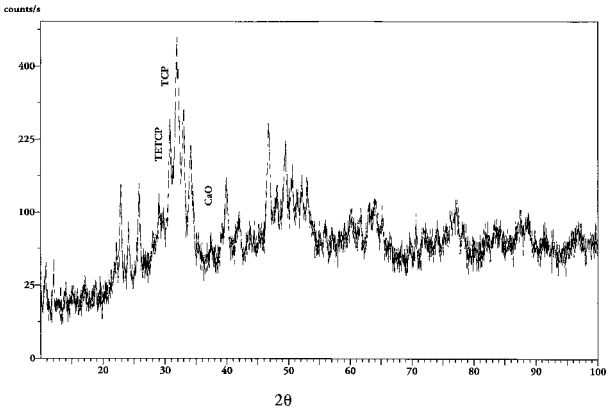

Figure 9 XRD recorded *in situ* of the coating material on the Ti plate prepared used 26 kW electrical input power (TETCP = $Ca_4P_2O_9$, TCP = α – TCP).

for the plasma-sprayed coating on the plate prepared at the highest electrical input power (26 kW). The most intense feature in the diffractogram was centered at $2\theta = 31.8°$(d = 2.81Å). This coincides with the (2 1 1) line expected for HAP. In general, the XRD pattern of the coating is dominated by features assoicated with an HAP phase. However, upon comparison with XRD from the commercial, high purity HAP powders and the HNO_3-digested-NaOH-reprecipitated cervine bone powders, additional features not related to HAP can be observed. These have been assigned to impurity phases that are known [18, 19] to form under the plasma-spraying conditions. Plasma temperatures depending on the gas used, can approach 20 000 °C. This is enough to partially melt outer diameters of the calcium phosphate feedstock particles (and stimulate phase transformations and decompositions) before they impact on the Ti substrate during the short residence time of the powder particles in the flame. From the XRD pattern given in Fig. 9, small amounts of three new phases appear to coexist with the bulk HAP plasma-sprayed coating. A peak of noticeable intensity observed at $2\theta = 30.7°$ (d-spacing 2.905 Å) corresponds to the most intense feature expected for α - $Ca_3(PO_4)_2$ (α-TCP) [10]. The second most intense peak for this phase coincides with an HAP-associated peak occurring at $2\theta = 34.2°$ (in Fig. 9 there is a broadening of this feature implying two overlapping components) and the third most intense peak of a α - $Ca_3(PO_4)_2$ occurs at $2\theta = 22.72°$. When comparing the XRD pattern in Fig. 9 with that for NaOH reprecipitated HCl-digested MIRINZ bone powder (see Fig. 2 (b)), a feature can be observed at $2\theta = 22.72°$ (in Fig. 9) that overlaps a weak HAP-associated feature. A much weaker peak just discernible at $2\theta = ca.\ 29.8°$ is coincident with the most intense peak expected for tetracalcium phosphate $Ca_4P_2O_9$ [10] and thus may be tentatively assigned to this phase. In addition, when comparing XRD patterns of coated plates prepared using low electrical input powers with those of plates prepared using higher input powers, a weak peak can be detected appearing at $2\theta = ca.\ 37.4°$ which corresponds to CaO [10].

The presence of these impurity phases in the plasma sprayed coatings can be understood by considering the transformation chemistry of the feedstock powder in the very high temperatures momentarily experienced by the

powders in the plasma. The as-received MIRINZ reprecipitated bone powder used a feedstock has an ICP-measured Ca : P ratio of 1.53 indicating that it represents a Ca-deficient HAP. It is known [19] that Ca-deficient HAP can transform upon heating to a variety of other products. At temperatures $< 900\,^{\circ}C$, it converts to HAP and β-tricalcium phosphate (β-TCP). β-TCP, itself, converts to α-TCP at temperatures $> 1100\,^{\circ}C$ and HAP decomposes above temperatures of $1300\,^{\circ}C$ to α-TCP and tetracalcium phosphate ($Ca_4P_2O_9$). Thus, in the plasma spray coatings prepared from the MIRINZ reprecipitated bone powder, the observation of α-TCP and small amount of ($Ca_4P_2O_9$) impurities can be readily understood in terms of the above chemistry. The observation of CaO in coatings prepared at higher electrical input powers also agrees with the work reported by McPherson *et al*. [18], who also detected $Ca_4P_2O_9$ in coatings by XRD. In general, it is desirable to minimize the formation of CaO in plasma sprayed coatings as (1) the CaO can react with water coming into contact with the coating and thus destroy adherence, and (2) CaO presence in the coatings is not desirable from a toxicity point of view especially if the coatings are to come into contact with body tissues.

3.12.2. SEM and energy dispersive X-ray analysis (EDX)

Fig. 10 is an SEM of a plasma coating prepared on a titanium metal plate from MIRINZ reprecipitated bone powder. In general, the coatings on all three plates showed three distinct microstructural features. The first was areas of glassy smooth ''splats'', which are features normally observed in plasma spray coatings [19]. The splats arise from the feedstock particles partially melting in the plasma, and deforming into characteristic amorphous disk-shaped plates as they impact on the titanium substrate surface. The second feature observed was the presence of various sized (0.2–100 μm) spherical particles. These arise because many of the partially molten particles retain their spherical morphology (as possessed in the original powdered state) as they become incorporated in the plasma coating, a fact also noted by McPherson *et al*. [18]. The third feature observed was areas of ''microcrystalline- appearing'' material (see Fig. 10) interspersed in various regions of the coating. These represent significantly finer particle sizes. There was little difference in microstructural characteristics across the three plates except for an apparently lower occurrence of spherical and microcrystalline-appearing material in the plates prepared at higher powers suggesting a greater proportion of meltdown of the feedstock in the higher power plasma.

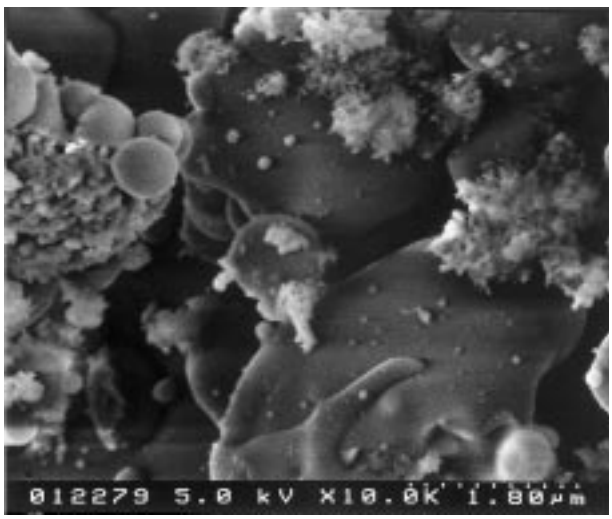

Figure 10 SEM of coating material on the plasma sprayed Ti plates showing typical features.

EDX analyses were performed over: (a) a general area of the plates, and (b) in localized areas corresponding to locations of splats, spherical particles and microcrystalline-appearing clusters of particles of the plates. EDX spectra of the coatings exhibited peaks due only to Ca, P and O and were clear of any other impurity elements. Ca : P ratios measured from the coatings are summarized in Table VI. The error in these is considered to be within $\pm$ 10% as expected for measurements of this type using SEM/EDX. All plates exhibited a molar Ca : P ratio that was higher (i.e. 1.79–1.88) than that expected for stoichiometric HAP (1.67). The estimated Ca : P ratios obtained from spot analyses carried out in areas where characteristic microstructural features (splats, spheres and microcrystalline clusters of particles) occurred varied very widely and showed that the 1.79–1.88 molar Ca : P ratio (from analyses over a more generalized area) represents an average of components of widely varying Ca : P molar ratios. The Ca : P ratio of 3.32 estimated by measurement of the Ca and P peak heights is particularly high and is evidence for a calcium rich CaO-P_2O_5 glass phase as postulated by McPherson *et al*. [18] in previous studies on plasma-sprayed HAP coatings.

3.12.3. Analysis of the scraped coatings by ICP and FTIR spectroscopy

In general, FTIR spectra of scraped material from the three plates prepared at different powers showed no significant spectroscopic differences between the three coatings. The dominant features of the spectrum were typical of that of an apatitic calcium phosphate phase and so similar to features observed in the FTIR spectra of the feedstock powder. However, it was evident that the fat and carbonate-associated IR peaks had disappeared presumably by decomposition of these components in the plasma coating process.

ICP analysis was conducted on the scraped plasma spray coating material in order to provide a check on the reliability of the *in situ* EDX-determined Ca : P ratios as discussed earlier. The results of these analyses are summarized in Table VII. Although, the elemental concentrations measured by ICP are higher than those measured by EDX, the Ca : P molar ratios are very similar (on average Ca : P are higher ratio = *ca*. 1.83) between the two methods of measurement. As ICP analysis is regarded as a superior method to EDX for measuring elemental concentrations, a greater degree of confidence is taken from these results. In general, the results show there is very little phase difference overall between the three coatings. It is apparent, however, that the Ca : P ratio has increased from that of the starting

TABLE VI Elemental composition of plasama-sprayed bone powder coatings by EDX analysis. Ca : P ratios for the spot analyses of the different structural components in the coatings (viz., glassy lamella, spherical particles and crystalline material) were estimated from the relative peak heights while the Ca : P ratios for the coatings (which were analyzed over a wider area) were obtained quantitatively using a certified HAP standard

Sample (power input)	O (%)	Ca (%)	P (%)	Ca : P molar ratio
Plate 1 (18 kW)	44.68	39.49	15.83	1.88
Plate 2 (22 kW)	45.71	37.93	16.36	1.79
Plate 3 (26 kW)	45.23	38.54	16.23	1.84
Glassy lamella				3.32 (estimate)
Spherical particles				1.30 (estimate)
Microcrystalline appearing material				1.20 (estimate)

TABLE VII Concentrations of Ca, P and Ti measured in plasma spray coatings scraped off a Ti plate as measured by ICP methods

Sample description	Ti (ppm)	Ca (%)	P (%)	Ca : P molar ratio
Plate 1 (18 kW)	280	39.0	16.5	1.83
Plate 2 (22 kW)	560	38.0	16.2	1.82
Plate 3 (26 kW)	490	37.0	15.6	1.84
As-received MIRINZ reprecipitated bone (feedstock) powder	n/a	27.5	13.9	1.53

n/a = Not applicable, Ti was not analyzed for in this sample.

material (Ca : P = 1.53) confirming that decomposition/transformation of the feedstock and occurred during coating. McPherson *et al*. [18] used stoichiometric HAP (Ca : P molar ratio = 1.67) as a feedstock material in their plasma coating studies, which gave resulting plasma-sprayed coatings with analyzed Ca : P molar ratios of 1.78–2.03 for power input settings ranging from 10 to 35 kW. Ti presence in the scrapings (Table VII) is due to mechanochemically bonded metal scraped off with the calcium phosphate coatings.

4. Conclusions

This study has shown that animal bone-derived calcium phosphate powders are a potentially useful source of materials for biomedical or nutritional purposes either in a milled form derived directly from boiling and crushing of the animal bones or as an acid-digested/reprecipitated form. It has been shown that the powders may be developed as enzyme immobilization substrates and that residual impurities in the bone such as collagen or fat enhance the adsorbent properties of the materials. Reprecipitated bone powders have also shown promise as a feedstock in plasma spraying on Ti substrates and thus represent an alternative source of calcium phosphate powder that could be cheaper than conventional chemically synthesized powders for these applications.

Acknowledgments

The authors would like to acknowledge the New Zealand Foundation for Research, Science and Technology (FRST) for a grant made from the Public Good Science Fund to cover the costs associated with this research. G.S.J. is grateful to MIRINZ Food Technology and Research for a scholarship provided for the tenure of the research project. The authors would also like to acknowledge Dr Bill Henderson of the University of Waikato Chemistry Department for advice on enzyme immobilization using phosphine coupling. Dr Roger Mederr of Forest Research is also thanked for recording solid state MAS ^{13}C and ^{31}P NMR spectra of the bone powders.

References

1. L. SAVARINO, S. STEA, D. GRANCHI, M. E. DONATI, M. CERVELLATI, A. MORONI, G. PAGANETTO and A. PIZZOFERRATO, *J. Mater. Sci: Mater. Med.* **9** (1998) 109.
2. P. FRAYSSINET, E. ASIMUS, A. AUTEFAGE and J. FAGES, *ibid.* **6** (1995) 473.
3. B. F. YETER-DAL, V. GROSS, and T. W. TURNEY in ''Ceramics, adding the value, Volume 2'' *Proceedings of the International Ceramic Conference, Australia, 1992*, (CSIRO Publications, Melbourne, 1992) p. 617.
4. Composition of Ceramic Hydroxylapatite for Surgical Implants, ASTEMF 1185–88.
5. G. S. JOHNSON, M. R. MUCALO and M. A. LORIER, *J. Mater. Sci: Mater. Med.,* in press.
6. *AOAC International 16th edn* (Association of Official Analytical Chemists), **2** (1995) Ch. 39, p. 7.
7. F. C. COCHRANE, H. H. PETACH and W. HENDERSON, *Enzyme and Microbial Technology*, **18** (1996) 373.
8. United States Pharmacopoeia (USP) Twenty First Revision (1985), United States Pharmacopoeial Convention Inc., Maryland, p. 1104.
9. S. KANO, A. YAMAZAKI, R. OTSUKA, M. OHGAKI, S. NAKAMURA, M. AKAO and H. AOKI, Apatite Volume 1, Proceedings of the First International Symposium on Apatite, Mishima, Japan, July 1991 (Japanese Association of Apatite Science, March, 1992) 91.
10. Powder Diffraction Files, Pattern numbers: 4–0777 (CaO), 5–0628 (NaCl), 25–1137 ($Ca_4P_2O_9$) and 9–348 (α - $Ca_3(PO_4)_2$) Joint Committee on Powder Diffraction Standards, Philadelphia, 1974.
11. W. KEMP in ''NMR in Chemistry, A Multinuclear Introduction'', (Macmillan Education Ltd, London, 1986) p. 217.
12. E. D. WEIL in ''Handbook of Organophosphorus Chemistry'' edited by R. Engel (Dekker, New York, 1992) Ch. 14.
13. W. HENDERSON, G. M. OLSEN and L. S. BONNINGTON, *J. Chem. Soc. Chem. Commun.* (1994) 1863.
14. H. H. PETACH, W. HENDERSON and G. M. OLSEN, *ibid.* (1994) 2181.
15. W. HENDERSON, H. H. PETACH and L. S. BONNINGTON, *Eur. Poly J.* **31** (1994) 981.

16. W. HENDERSON, Chemistry Department, University of Waikato, Private Communication.
17. J. EVERSE, C. L. GINZBURGH and N. O. KAPLAN in ''Methods of Biochemical Analysis'' edited by C. Suelter, (Wiley, New York, 1981) p. 135.
18. R. MCPHERSON, N. GANE and T. J. BASTOW, *J. Mater. Sci: Mater. Med.* **6** (1995) 327.
19. L. HENCH and J. WILSON in ''An Introduction to Bioceramics, Advanced Series in Ceramics-Vol. 1'', (World Scientific, Singapore, 1993) p. 154, 199.

Received 25 February 1999
and accepted 26 January 2000